Final Technical Report
USGS Cooperative Agreement for Geodetic Monitoring Operations:

Award G10AC00145

Continuous Broadband Monitoring of Crustal Deformation Near Active Faults in Southern California

3/01/2010 — 2/28/2015

Duncan Carr Agnew
dagnew@ucsd.edu (858) 534-2590

Frank K. Wyatt
fwyatt@ucsd.edu (858) 534-2411

Institute of Geophysics and Planetary Physics 0225
University of California San Diego
9500 Gilman Dr, La Jolla, CA 92093-0225

1. Major Goals and Activities of the Geodetic Project

This grant helped support the operation of two facilities for the continuous measurement of strain changes in southern California: Piñon Flat Observatory (PFO), between the San Jacinto and San Andreas faults, and at Durmid Hill (DHL), near the southern end of the San Andreas fault, and effectively within the fault zone. The USGS-supported instruments at these locations – a single longbase strainmeter at DHL (augmented by an orthogonal PBO-sponsored strainmeter), and three strainmeters and one longbase tiltmeter at PFO – measure crustal deformation in Southern California for periods from seconds to years. **Figure 1** shows the locations of these strainmeters, along with the new ones (as green dots) that have been added by the Plate Boundary Observatory (PBO) project as part of Earthscope. By recording strain over this wide range of frequencies these measurements provide a nearly unique bridge between seismology and geodesy that is otherwise rarely available. This award supported power, network connectivity, instrument maintenance and operation, data recording, preliminary data-processing, and data distribution.

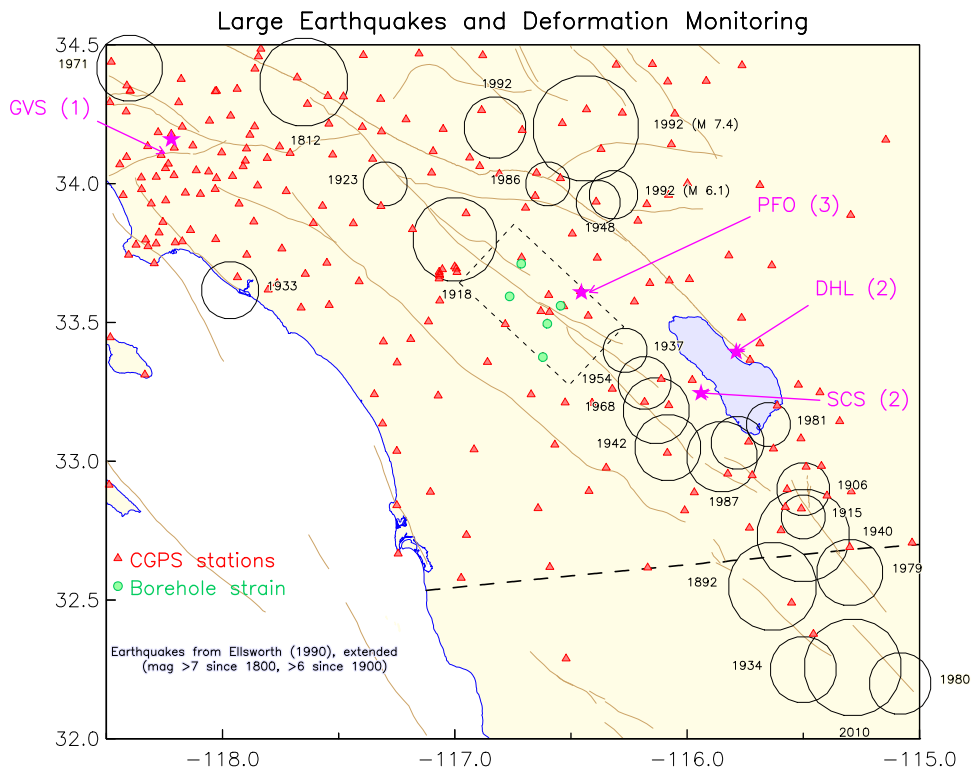

Figure 1: Large earthquakes and fault ruptures in southern California, with locations of laser strainmeters (purple), borehole strainmeters, and GPS. The dashed box is the ‘‘Anza gap’’.

Over the last eight years a pattern of aseismic strain transients has been observed in the long-term strain data from the PFO LSM’s. These transients follow some (but not all) episodes of strong shaking and large dynamic strain either from local earthquakes of magnitude around 5, or larger regional shocks. Wdowinski (2009) suggested that since, on the San Jacinto fault, the

transition from earthquakes to creep below the seismogenic zone is relatively shallow, such creep could well include unsteady deformation – which we believe the PFO measurements are recording. We have also observed transients, probably from shallow creep events, on the DHL LSM's.

2. Accomplishments

2.1. Operations

The primary activity throughout the period of the grant was sustaining high quality recordings at the field sites; over the course of the year, we averaged 1–2 trips per month to both sites to deal with immediate issues (the reason for the majority of responses) and for planned preventive care. Time in the lab was spent on repairs, data processing, and evaluating and understanding the recordings. All of this paid off in very low downtime (Table 1).

Table 1: Downtime of LSM Channels

Site	Comp.	Channel	2006	2007	2008	2009	2010	2011	2012	2013	2014
PFO	NS	**Main**	**4.7**	**11.5**	**6.5**	**1.4**	**4.4**	**3.9**	**2.4**	**0.3**	**0.4**
		Local Anch.	3.2	1.6	0.6	4.7	5.9	7.6	0.4	10.8	0.8
		Remote Anch.	1.9	2.7	0.7	2.1	1.9	0.6	0.4	0.3	1.2
	EW	**Main**	**5.1**	**4.5**	**1.6**	**2.1**	**3.3**	**3.3**	**3.2**	**0.7**	**0.1**
		Local Anch.	1.6	2.9	1.5	0.8	1.6	1.2	3.5	3.3	1.1
		Remote Anch.	2.9	2.0	3.7	2.8	2.4	4.1	2.0	5.8	0.1
	NW	**Main**	**2.7**	**5.5**	**1.3**	**1.5**	**1.3**	**3.4**	**3.5**	**1.7**	**1.8**
		Local Anch.	1.6	6.8	3.9	1.5	5.3	0.8	2.2	2.1	0.8
		Remote Anch.	8.7	4.2	1.0	1.4	0.8	0.3	1.2	1.3	0.2
DHL	NS	**Main**	**4.9**	**0.9**	**3.4**	**0.4**	**5.0**	**1.8**	**2.2**	**1.3**	**1.7**
		Local Anch.	2.8	0.8	2.6	0.4	8.7	0.5	0.6	1.2	0.9
		Remote Anch.	2.5	0.2	1.1	1.1	4.7	3.8	0.1	6.5	1.1

All values are percent.

A secondary activity was helping to support other investigators and other projects using the PFO facility. Table 2 provides a summary.

Table 2: Other Investigations at PFO

Univers. Bath	T. Whitley	Atmospheric 'sprite' monitoring
Caltech	J.-P. Ampuero	Operation of a small, dense, seismic array to search for tremor on the San Jacinto fault.
UCSD	M. Zumberge, J. Berger	Testing new optical-fiber borehole seismometers.
UCSD	M. Zumberge, F. Wyatt	Testing a surface fiber-optic strainmeter parallel to one of the PFO strainmeters, and a vertical fiber-optic borehole strainmeter.
Tech. Univers. Munich	U. Schreiber	Ring-laser seismometer recording.
Wash. Univers. St. Louis	R. Cowsik, T. Madziwa-Nussinov	Testing a new type of rotational seismometer.

LSM operations at PFO have been supported over the years by a range of agencies. Over the last 15 years the majority of the support came from the USGS's funding of geodetic and seismic monitoring as part of NEHRP, with important additional contributions by SCEC, and by

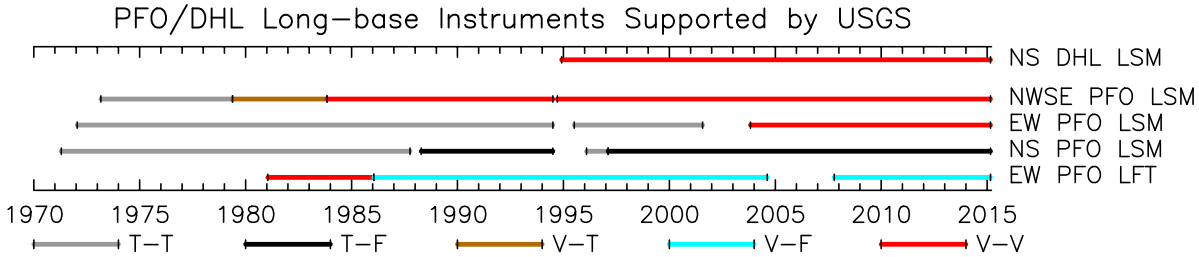

Figure 2: Time spans of data from PFO and DHL longbase instruments. Colors refer to anchoring (at the two ends): from worst to best, T for pier tilt, F for optical fiber anchor, V for vacuum-pipe anchor. Thus, of the PFO LSM's, we give the most weight to the NWSE, followed by the EW and the NS.

UCSD matching funds, though after 2008 the latter were greatly reduced because of University budget cuts. Other users of the PFO facility also have provided small amounts to help maintain it

2.2. Aseismic Strain Events on the San Jacinto Fault

Unsteady (but slow) slip variations on faults are plausible, but have not often been observed on strike-slip faults (other than surface creep), and it remains unclear just how common they are. To see them we need data that has:

A. Low noise at the relevant long periods (see Section 1.1.1).

B. Proximity to the source, because the signal is dominated, not by radiated seismic energy, but by near-source terms that decay as r^{-2} (r^{-3} for strain).

C. A long time span: just as for earthquakes (and practically every other natural phenomenon) large events are rarer than small ones, and may be infrequent relative to the funding cycle.

Only after instrumentation satisfying (A), namely continuous GPS, was operated near subduction zones (B) for several years (C) was it seen that many zones have slow slip events (SSE's): in the last 20 years, SSE's have moved from unknown to rare to (at most) uncommon – there are still many uninstrumented regions. For strike-slip faults such events might be smaller or less frequent, since the depths at which such behavior is expected correspond to a much smaller area on a vertical plane than a shallowly dipping one. But it is also true that few such faults have had the necessary instrumentation for long spans of time: for the San Andreas and San Jacinto faults, only the regions around San Juan Bautista, Parkfield, and Anza (Agnew 2007). Slow slip events have been observed in the first two, (Linde *et al.* 1996, Langbein *et al.* 1996, Uhrhammer *et al.* 1999), both of which are unusual in being transitions from creeping to locked parts of the fault, with (perhaps) no large earthquakes. The Anza area is more typical, in having no surface creep, and a clear paleoseismic record of large events; and we believe that the LSM data provide good evidence for both triggered and (less definitely) spontaneous episodes of slow slip at seismogenic depths.

2.2.1. Triggered Events

We have observed six similar episodes of rapid strain change at PFO following most of the large regional, or smaller local, earthquakes listed in Table 1. We can observe these episodes and see their similarity because PFO has been operating for a long time, and also because the most

Table 3: Significant Ground Motion at PFO

Date	Mag	Dist (km)	Pk. Acc. (cm^2/s) N	U	E	Pk Vel (cm/s) N	U	E	Name
1980:056	5.3	15	109	49	124				Horse Canyon
1992:114	6.1	44							Joshua Tree
1992:180	7.3	66	25	26	48	2.0	5.2	2.9	Landers
1999:289	7.1	111	26	21	35				Hector Mine
2001:304	5.0	21	132	109	120	2.3	1.2	3.6	Anza
2005:163	5.2	21	309	219	273	5.7	3.5	7.3	Anza
2010:094	7.2	185	13	14	13	3.7	2.4	2.4	El Mayor
2010:188	5.4	25	182	99	107	3.7	1.9	2.2	Collins Vly
2013:070	4.7	15	44	109	60	1.2	1.0	1.7	Toro Pk

Peak ground motion (absolute value) from earthquakes that caused strong shaking at PFO: blanks indicate that information is not readily available.

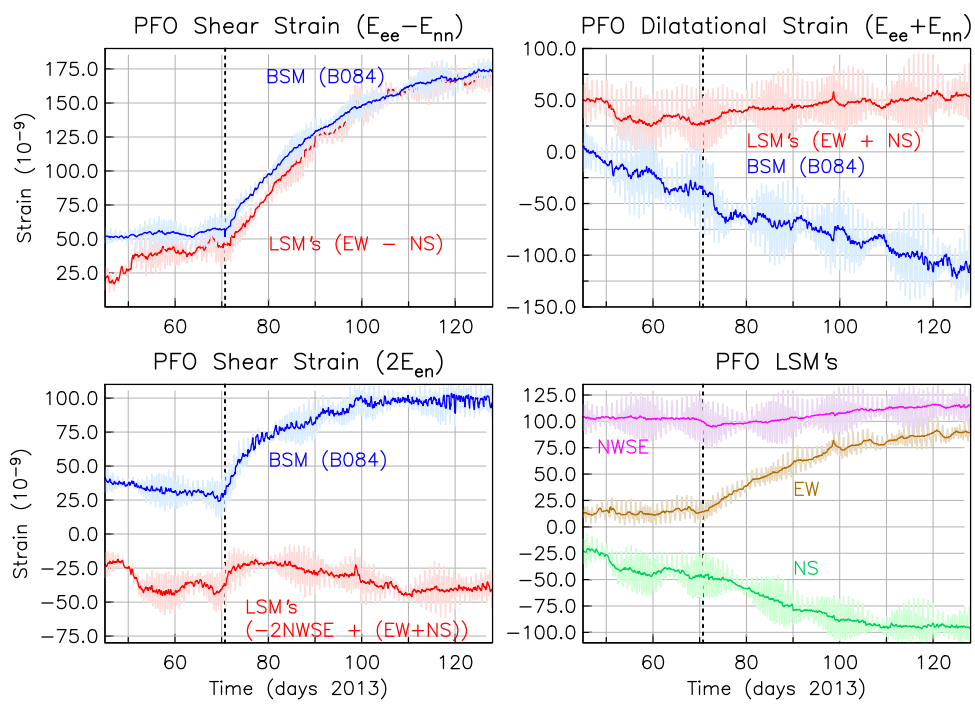

Figure 3: Areal strain and two components of shear at PFO, showing the postseismic behaviors of the LSM's and BSM's after the 2013 Toro Peak earthquake (dashed black line). Only the BSM data (calibrated using Hodgkinson *et al.*, 2013) are detrended; in the detided records S_1 and S_2 variations have been removed from the BSM areal strain and from all the LSM data. The lower right panel shows the individual LSM records.

recent decades have been more seismically active. From 1938 through 1996 the Anza region experienced six shocks with $M > 4.5$, and only one with $M > 5.0$; for 1997-2014 there have been another six shocks with $M > 4.5$, and three with $M \geq 5.0$ (Felzer and Kilb 2009).

We begin (**Figure 3**) with the most recent aseismic event, which followed what we call the "Toro Peak" earthquake, on March 11, 2013 (2013:070:16:56), M 4.7, 9 km deep and 12 km

south of PFO (15 km total distance). While the LSM's lost fringe lock for about a minute during the high accelerations, they show all other strain changes, including a rapid postseismic change. Combining the NS and EW LSM records to form two of the strains usually computed for the BSM's showed fairly good agreement between these and the strains recorded by the PBO BSM (B084) at PFO, which is within the region covered by the LSM's. The strain changes agree best for the $g1$ shear (the shear parallel to a NWSE-striking fault) and the areal strain ea, though not so well for the $g2$ strains, something that may reflect calibration errors in the BSM. Except in the lower right panel the strains in **Figure 3** are all derived from combinations of sensors. For shear this reduces common-mode noise in the BSM's, though combining the LSM's often increases the apparent noise over that of an individual sensor.

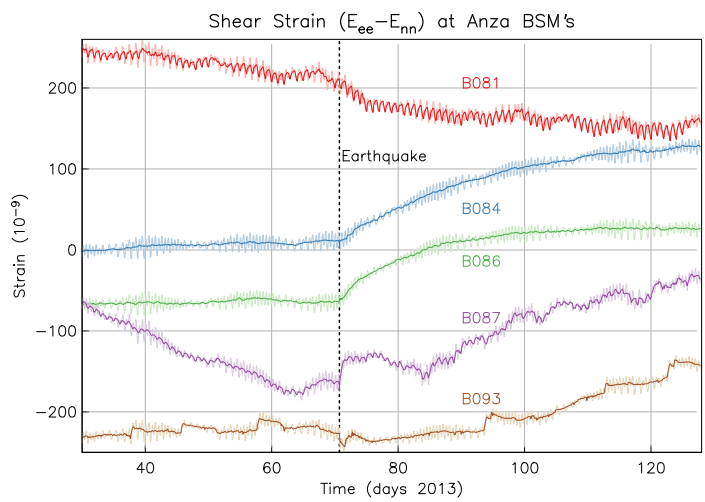

Figure 4: Fault-parallel shear from Anza BSM's, using the fully-corrected PBO time series.

Seismic data (examined by the USGS and Caltech) showed no signs of tremor, nor were any fluctuations seen on continuous GPS data: not surprising, since the strains observed, even if uniform over 20 km, would given displacements less than 2-3 mm. Additional data come from the other PBO BSM's in the Anza region (located in **Figure 3**); we omit B088 and B946, which had shown unstable behavior. **Figure 4** shows estimated $g1$ strain for the remaining sensors: some, but not all, show the same decaying postseismic signal seen at PFO.

We can rule out instrument misbehavior: the NS and EW LSM's at PFO have no elements in common, and the BSM is completely independent of the LSM's. We can also rule out weather effects, since the weather was benign, with no rain or large air pressure changes. These observed strain changes have to be in the ground. We know (Evans and Wyatt 1984) that hydrological changes at the NW corner of PFO cause displacements of all three LSM ends; but such changes are unlikely to displace the W and N ends in equal and opposite ways and the NW end not at all – and it is even more unlikely that such a localized source could produce the same strains at the BSM, 400 m away and 150 m deep. Indeed, the agreement of the PFO LSM's with the BSM implies that the scale of the strain must be considerably greater than the LSM baselength of 720 m, and it is difficult to see how a hydrologic change of this scale could have, in such relatively impermeable rocks, a time constant as short as a few weeks. Finally, broad-scale hydrological

change would affect the water table at PFO, but no change was seen either in three water-level monitoring wells or in pore-pressure data from the B084 borehole.

Further evidence against some sort of local response to shaking is provided by the Collins Valley earthquake, three months after the EMC shock (Table 1) This produced peak accelerations and velocities (a proxy for strain) comparable to other events at PFO, but did not create a comparable response (**Figure 5**). Avouac *et al.* (2014) have used BSM and seismicity data to argue that deep slip was triggered by this event. Comparisons with the LSM data for this and other events will be valuable; we are providing their group with early LSM data not yet in the IRIS DMC.

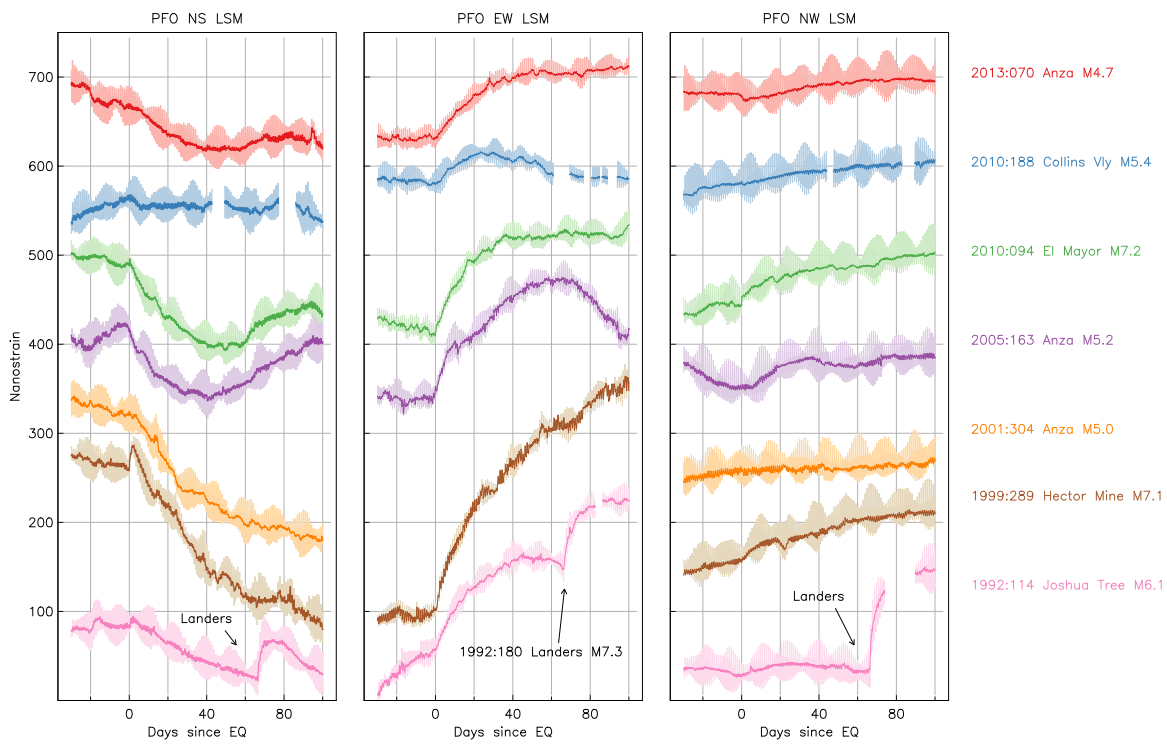

Figure 5: Responses of the three PFO LSM's to eight earthquakes, four local and four regional (Table 1). The EW LSM was being rebuilt at the time of the 2001 earthquake.

We recognized the 2013 postseismic strains as being similar to those we had observed after the 2005 Anza earthquake and the 2010 El Mayor Cucapah (EMC) earthquake. The latter was particularly interesting, since for a few hours after the mainshock the LSM's showed postseismic strain changes roughly consistent with afterslip on the EMC-related fault; but then the strain rate changed dramatically, even changing sign on the NS LSM, to the same pattern seen in 2005 and 2013.

In the 2005, 2010, and 2013 events there was relatively little change on the NWSE strainmeter. Since for a long time this was the only fully-anchored LSM (**Figure 1**) it has been the one we put the most weight on, especially for longer-term changes. Looking back, we see that pattern of postseismic strains after Anza earthquakes in 2005 and 2013, and after the EMC earthquake in 2010, also occurred after the 1992 Joshua Tree, 1999 Hector Mine, and 2001 Anza earthquakes. **Figure 5** shows all these, along with two times that the pattern was not observed:

after the 2010 Collins Valley earthquake (see above), and after the 1992 Landers earthquake, which produced a much larger, but very different, postseismic response.

So we find a repeated pattern of strain change at PFO after either moderate local shocks or larger and more distant ones. For the reasons given above we rule out purely local deformation, leaving, as the most likely source, aseismic slip on the San Jacinto fault.

We can use the PFO data to estimate the slip location. Slip at any specific location on the fault will produce particular ratios between observed strains; given observed ratios we can find possible source regions, and with enough ratios limit this to one part of the fault. More formally, given any set of N observed strain changes, we scale them to create an N-dimensional unit vector bah, which preserves the ratios. We can likewise associate a unit response vector $bbh(bx)$ with slip (of a specified rake) at any location bx on the fault. The misfit between bah and bbh is the angle between them which is given by the dot product $bah \cdot bbh$, which is one for a zero angle. Requiring this dot product to be more than some amount gives the region on the fault plane for which the slip would satisfy the data.

To apply this to slip on the San Jacinto fault in the Anza area, we assume right-lateral slip on a plane dipping at 82°. We estimate the net changes for the 2005, 2010 EMC, and 2013 earthquakes from the data in **Figure 5**; acceptable regions are those with an angle between unit vectors of 15° or less. Only small regions on the fault can produce strain changes with the observed ratios; since the ratios are similar, the acceptable regions are in much the same place – though the slip in 2005 and 2013 is less constrained in depth than that in 2010. The locations are mostly at the SE end of the seismicity gap near the town of Anza.

By taking the slip location to be the point that maximizes the product $bah \cdot bbh$, we can estimate the moment release. If we assume identical locations for the 2005 and 2010 sources, each has a moment of 1.8×10^{17}N-m, or $M_w ee 5.5$, and produce displacements of only 1.6 mm horizontal and 2.0 mm vertical on the nearest continuous GPS stations. If the 2005 event is 20 km deep (its best-fitting location) its moment is $M_w ee 5.9$.

2.2.2. Long-Term Strain Changes at PFO

To set these strain episodes into context, **Figure 6** shows data from all three LSM's at PFO from the start of 1999 to the end of 2014. The postseismic responses from **Figure 7** (except of course for the 1992 Joshua Tree shock) are highlighted in pink.

In looking at the longer-term strains we rely most heavily on the NWSE LSM (red trace), as the most well-anchored. In late 2010 this showed a fairly abrupt shift to compressional strain, in an episode lasting for almost a year, highlighted in green in **Figure 6**. At the same time, the EW LSM, which generally shows the expected long-term extension, also went into compression. Analyzing this as we did the postseismic signals, we can again find a possible range of sources on the fault; this is shown (black polygon) in **Figure 3**, a source SE of, and possibly deeper than, that of the postseismic strains.

In **Figure 6** we have also highlighted two other times of possibly anomalous compression on the NWSE LSM; anomalous because, except for a year following the Landers earthquake, this instrument showed steady extension from 1985 through 1999 — a very long period of marked steadiness. The most interesting of these two episodes is the one that began in early 2004, and

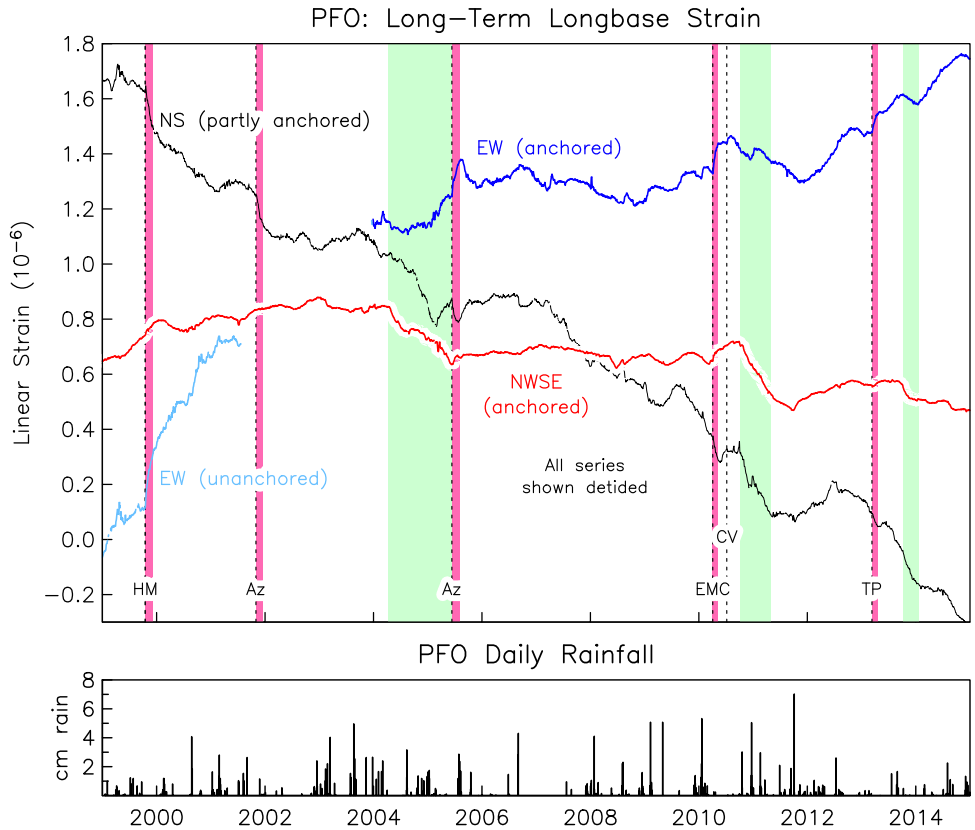

Figure 6: The last fifteen years of LSM data at PFO, with earthquakes from Table 1: HM for Hector Mine, Az for Anza (2001 and 2005) EMC for El Mayor Cucupah, CV for Collins Valley, TP for Toro Peak. Shaded regions show times of postseismic strain (pink) and possible anomalous strain (green).

ended at the time of the Anza earthquake in 2005. A tentative location is tantalizingly close to the aftershock zone of this event; the slip amount would be, very roughly, comparable to M_w between 5½ and 6. From this one example it not possible to establish a causal connection, but it does suggest that such relationships may exist on strike-slip fault segments and merits further investigation – which can only be done with more data.

We can also estimate a time series of strain in the broader Anza area using local CGPS stations (PBO and other; see **Figure 7**); this shows a somewhat earlier, and different, year-long postseismic response to the EMC event, with no dilatation. However, the GPS is averaging over a large area, and so is less sensitive to a locally-induced strain than the LSM's are. Unfortunately signals with this long a time constant cannot be reliably recovered from the BSM data.

2.3. Results of DHL Measurements

DHL is deliberately very close to the ''overdue'' section of the San Andreas fault, and also close to where this section meets the northern extension of the Brawley Seismic Zone. The seismicity of this part of the San Andreas is very low, though the geomorphic expression of the fault is extremely clear. Again, geodetic measurements show nearly pure shear, with total motion of about 25 mm/yr, and there is known surface creep, often triggered at the times of large

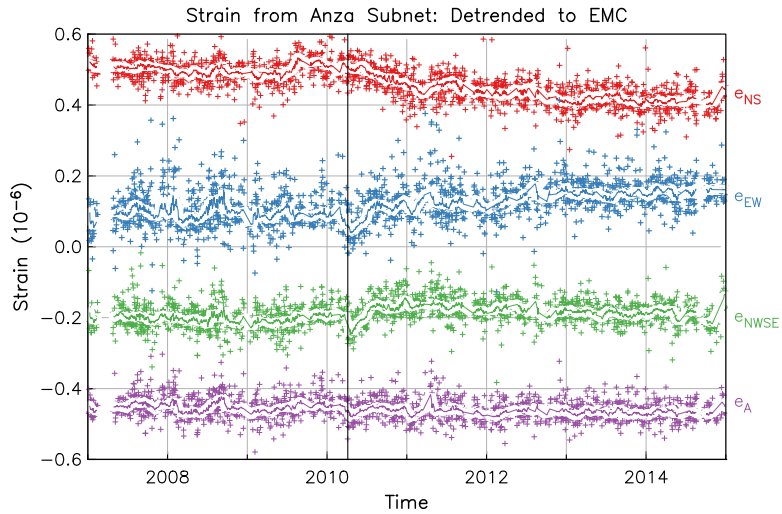

Figure 7: Daily strains computed from the displacements of continuous GPS stations DSSC, P479, P484, P490, P741, P742, and PIN1; **Figure 3** shows the region covered. Secular trends before the EMC earthquake has been removed; in $\mu\varepsilon$/yr, these trends are -0.13 for NS strain, 0.14 for EW strain, 0.01 for NWSE strain, and 0.005 for areal strain. The line shows a one-month robust smoothing.

earthquakes; we discuss examples of this below. DHL is on a large, gentle topographic uplift known as Durmid Hill; the local geology is interbedded claystones and siltstones, much deformed and only weakly cemented together.

The first impetus towards work in the area came with the 1988 identification of this section of the San Andreas as having the next-highest probability (after Parkfield) of producing an earthquake in the next 30 years; a subsequent study (Jones *et al.* 1991) suggested that more monitoring was needed. In 1991 we proposed a single LSM, which began unanchored operation in early 1994, and has been anchored since late 1994. A second LSM orthogonal to the first was funded by PBO, and has been operating since 2005.

Figure 8 shows the complete dataset from the two fully-anchored strainmeters at DHL. The (nearly) NS instrument (the one supported by this request) has a long-term rate of strain comparable to those estimated by interpolating GPS station velocities; so we conclude that this strainmeter is recording the secular strain; we believe the same of the newer (EW) PBO instrument, although its higher rate implies that there is steady dilatation at this site.

Both strainmeters show offsets from aseismic events, these usually last less than an hour. The 1999 events were also recorded on a temporary (NSF-sponsored) LSM then running at DHL, so we are sure these were not instrumental artefacts; we also believe the events in 2003 to be real. Section 1.4.5 discusses more recent aseismic events.

Having two instruments at this location is essential to validating that events show true earth deformation and to constraining possible sources. A recent example is the event on the PBO (EW) system at the start of 2010. Since this appears only on that system we are sure that it is not tectonic, but rather comes from rainfall that caused water to run near the instrument; some regrading has eliminated this problem.

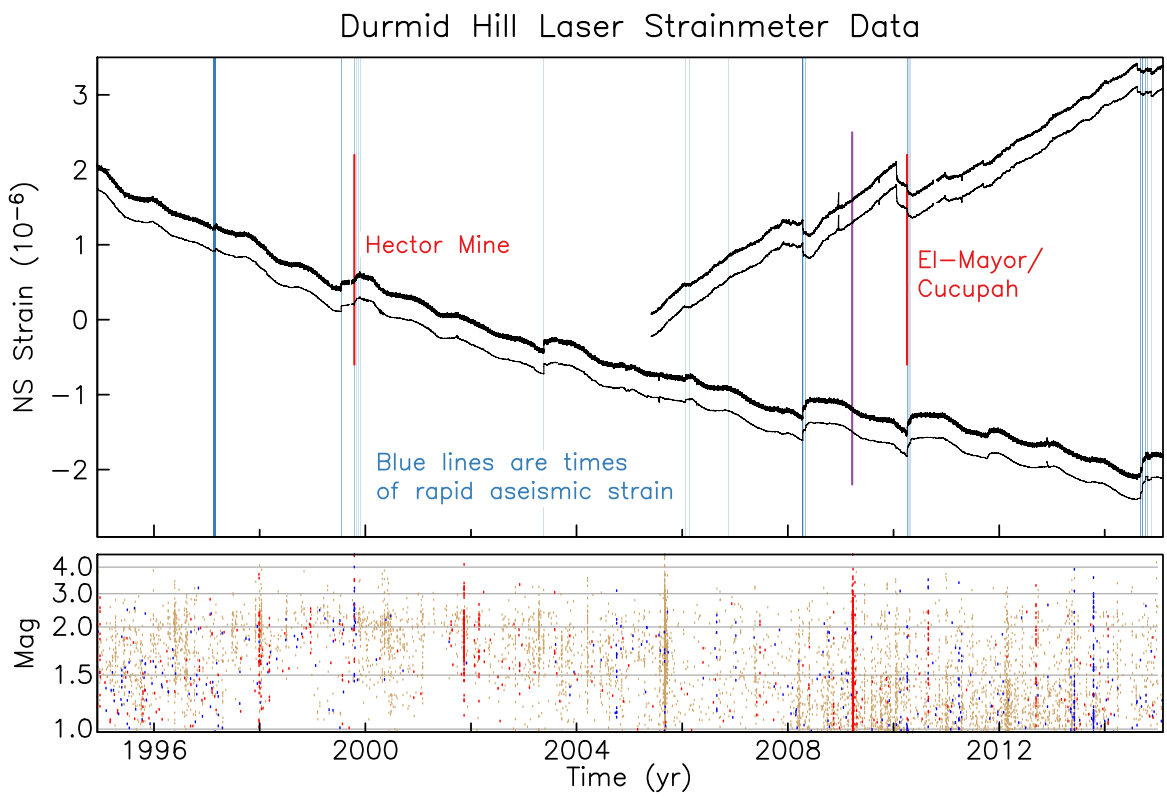

Figure 8: Data from the NS USGS (lower) and EW PBO (upper) LSM's. Traces are shown with and without tides. Red lines are times of major earthquakes, Purple line is time of swarm in 2008, which was not accompanied by any anomalous strain.

Figure 9 is an attempt to isolate the longer-term changes through three stages of processing. The first is to remove all the sudden strain changes just referred to. The second is to make a parabolic fit to the data; it is clear that a linear fit would not match the strain-rate changes seen. And the third is to isolate and remove seasonal cycles using the STL method developed by Cleveland *et al.* (1990).

The seasonal cycle is dominated by an annual sinusoid with amplitude 34 nε with a maximum on day 102; this is nearly in quadrature with the ground temperature at a depth of 1.2 m, which has an amplitude of 4.23° and is largest on day 204. We do not yet know whether this cycle comes from thermoelastic deformation, or (quite possibly) incomplete correction of end-motion by the fiber anchors; certainly, compared to any other near-surface strain record the annual cycle is small.

Once the annual cycle is removed, it is not clear if any of the series in **Figure 9** display significant changes. The one definite change, which is quite difficult to explain, is the secular change in strain rate, which appears to have decreased by a factor of more than between 1994 and the present. Unfortunately the time-span over which dense GPS coverage is available is much shorter; only since 2006 have there been even five stations within 20 km.

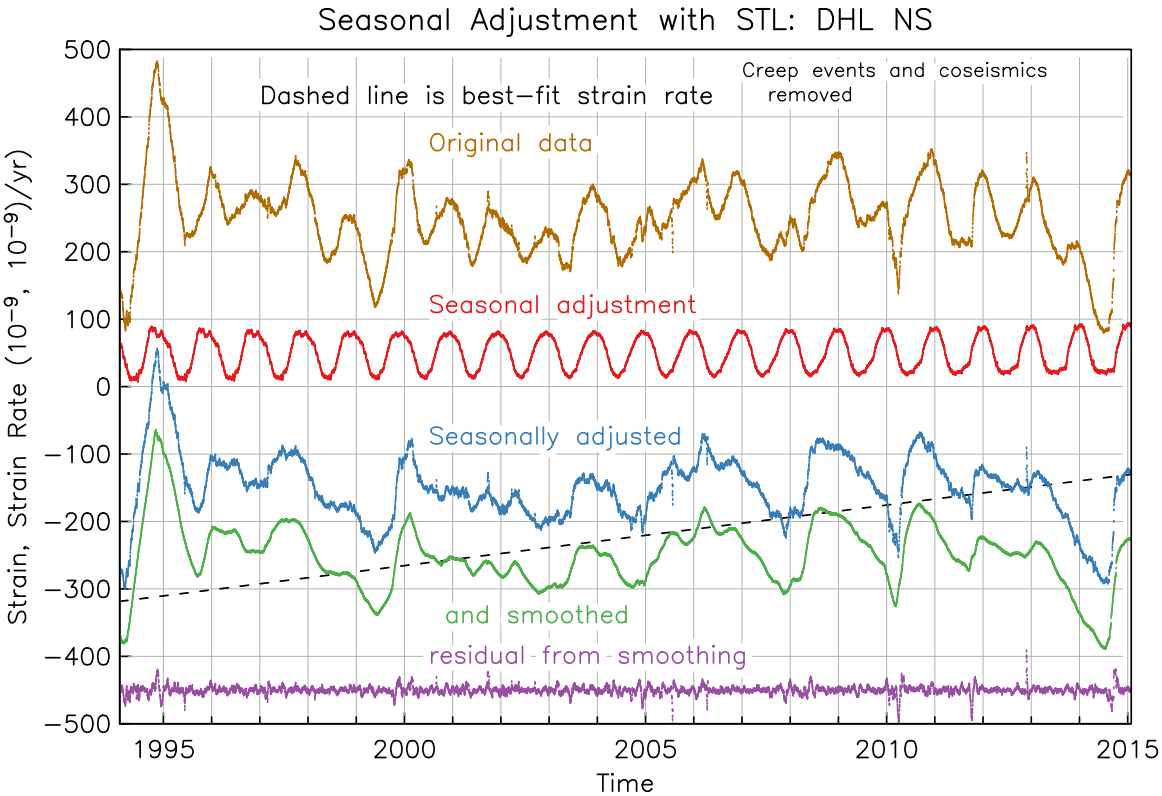

Figure 9: Long-term strain on the DHL NS strainmeter, after (1) removing all aseismic transients; (2) removing a parabolic fit (a rate change that is linear in time, shown by the dashed line). This gives the top trace; the seasonal component is plotted next, and then the residual after removing this. The two bottom traces show this residual decomposed into long-term and short-term fluctuations.

Figure 10 and **Figure 11** show the most recent set of rapid aseismic strains observed at DHL: 15 events in all between day 248 and day 321. It is notable that the ratio of strain change in these events on the two strainmeters is quite variable. This implies that the source regions must be different, and if they are in fact close to each other there are only a few locations on the San Andreas fault where they could be located, all fairly shallow.

Fortunately in this case we have additional information from a creepmeter operated by Prof. Roger Bilham on the San Andreas fault nearby. Comparing data from this with the LSM data (**Figure 11**) shows that while the creep events begin at the same time as the strain changes, they have much longer time constants, something strongly suggestive of diffusion from the source region to the surface.

There may have been seismicity related to this, since the Southern California Seismic Network reported a shallow magnitude 1.0 event about 1 km from the strainmeter on 2014:329:19:35:11 (Nov 25) at 33.393°N 115.781°W, depth 0.9 km. However, this event no longer appears in the SCSN or SCEC Data Center catalogs; it may have been a mis-association.

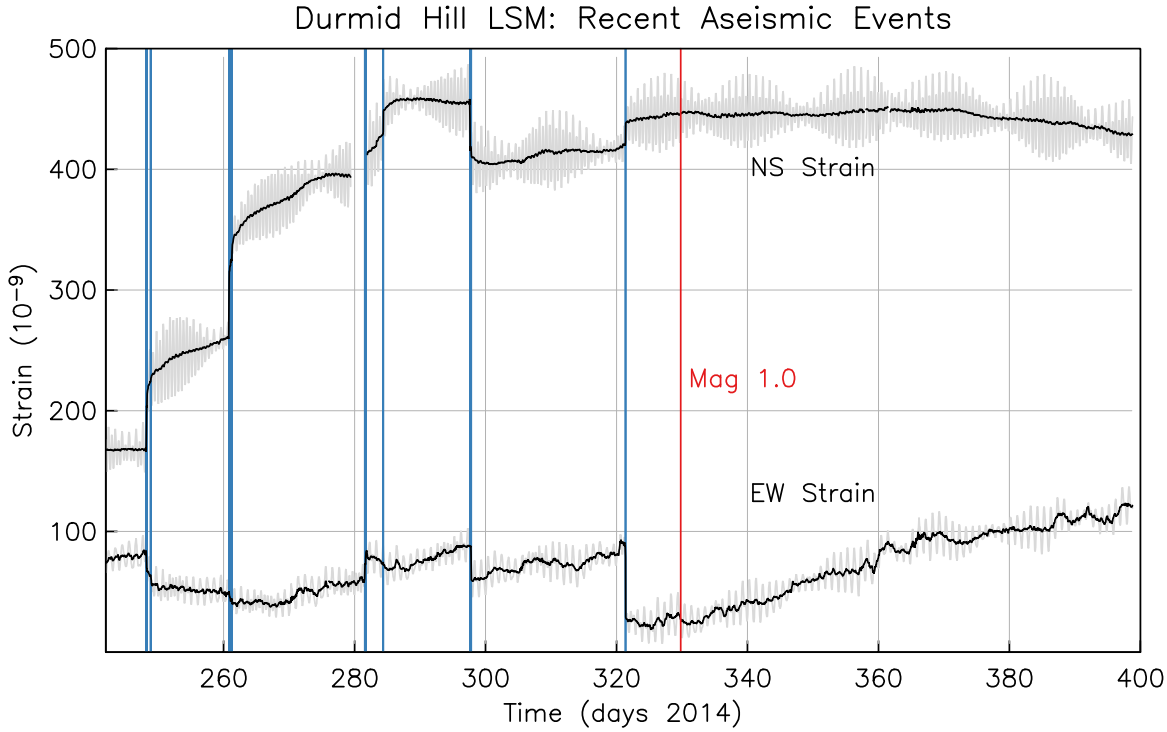

Figure 10: Most recent series of aseismic events at DHL, September through November 2015. Individual events shown by blue lines. Note the wide variability of relative amounts of strain offset.

Figure 8 suggests that these events may be associated with a rate change lasting into early 2015, with both the NS and EW instruments having lower rates than before. Without further data (past the end of this funding period) it would be difficult to decide.

3. References

Avouac, J.-P., A. Inbal, and J. Ampuero (2014). *Seismic and aseismic slip on the San-Jacinto fault near Anza, CA, from joint analysis of strain and aftershock data*, (San Francisco: Amer. Geophys. Union Fall Mtg.)

Evans, K., and F. Wyatt (1984). Water table effects on the measurement of earth strain, *Tectonophys.*, **108**, 323-337.

Felzer, K. R., and D. Kilb (2009). A case study of two M5 mainshocks in Anza, California: is the footprint of an aftershock sequence larger than we think?, *Bull. Seismol. Soc. Am.*, **99**, 2721-2735, doi:10.1785/0120080268

Hodgkinson, K. M., J. Langbein, B. Henderson, D. Mencin, and A. A. Borsa (2013). Tidal calibration of plate boundary observatory borehole strainmeters, *J. Geophys. Res.*, **117**, A114??, doi:10.1029/2012JB009651

Jones, L. M., K. E. Sieh, D. Agnew, C. Allen, R. Bilham, M. Ghilarducci, B. Hager, E. Hauksson, K. Hudnut, D. Jackson, and A. Sylvester (1991). Short-Term Earthquake Hazard

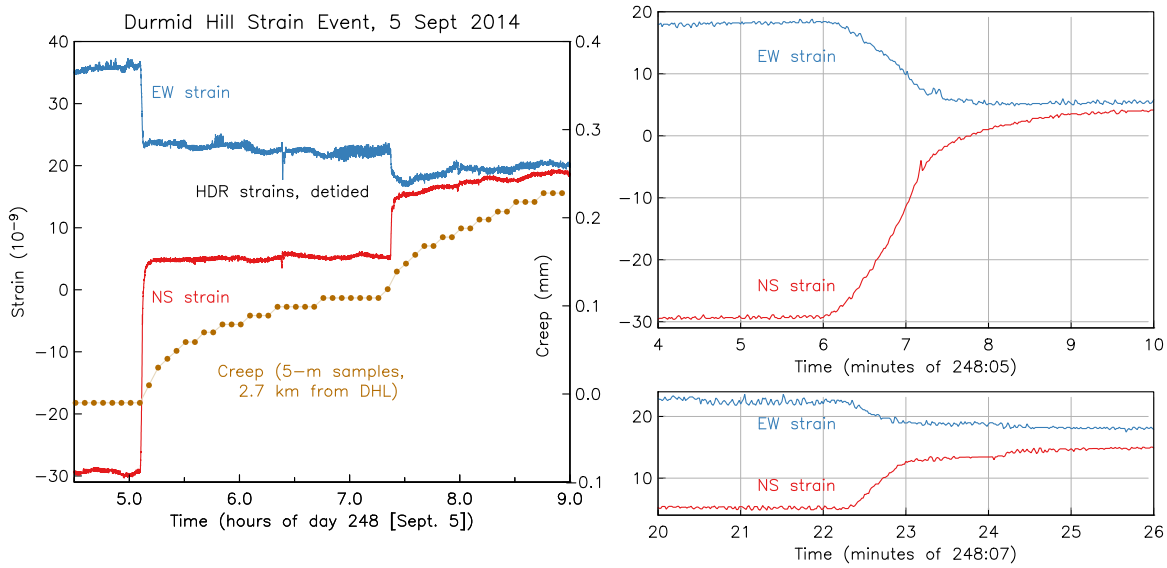

Figure 11: Expanded view of two aseismic events on 2014:248. Left panel shows the strains along with data from a creepmeter that crosses the San Andreas fault 2 km away (data courtesy of Prof. Roger Bilham). The two right panels show the strain from the two events on an expanded time scale.

Assessment for the Southern San Andreas Fault, Southern California, *U. S. Geol. Surv. Open-File Rep.*, **91-32**, A114??.

Langbein, J., R. L. Gwyther, R. H. G. Hart, and M. T. Gladwin (1999). Slip-rate increase at Parkfield in 1993 detected by high-precision EDM and borehole tensor strainmeters, *Geophys. Res. Lett.*, **26**, 2529-2532.

Linde, A. T., M. T. Gladwin, M. J. S. Johnston, and R. L. Gwyther (1996). A slow earthquake sequence on the San Andreas fault, *Nature*, **383**, 65-68.

Uhrhammer, R., L. S. Gee, M. Murray, D. Dreger, and B. Romanowicz (1999). The Mw 5.1 San Bautista, California Earthquake of 12 August 1998, *Seismol. Res. Lett.*, **70**, 10-18.

4. Publications Resulting from the Work Performed

Agnew, D. C., and F. K. Wyatt (2014). Dynamic strains at regional and teleseismic distances, *Bull. Seismol. Soc. Am.*, **104**, 1846-1859, doi:10.1785/0120140007

Barbour, A. J., and D. C. Agnew (2012). Detection of seismic signals using seismometers and strainmeters, *Bull. Seismol. Soc. Am.*, **102**, 2484-2490, doi:10.1785/0120110298

Wang, T-H., E. Cochran, D. Agnew, and D. Oglesby (2013). Infrequent triggering of tremor along the San Jacinto fault near Anza, California, *Bull. Seismol. Soc. Amer.*, **103** , 2482-2497, doi:10.1785/0120120284